Redox Biology 55 (2022) 102410

Contents lists available at ScienceDirect

Redox Biology

journal homepage: www.elsevier.com/locate/redox

Transfer of H_2O_2 from Mitochondria to the endoplasmic reticulum via Aquaporin-11

Ilaria Sorrentino [a], Mauro Galli [b], Iria Medraño-Fernandez [c,**], Roberto Sitia [a,*]

[a] Division of Genetics and Cell Biology, Istituto di Ricovero e Cura a Carattere Scientifico (IRCCS), Ospedale San Raffaele, Università Vita-Salute San Raffaele, 20132, Milan, Italy
[b] Department of Medical Biology, Medical University of Białystok, 15222, Białystok, Poland
[c] Department of Bioengineering and Aerospace Engineering, University Carlos III of Madrid, 28911, Madrid, Spain

ARTICLE INFO

Keywords:
Hydrogen peroxide
Redox homeostasis
Interorganellar crosstalk/ peroxiporin
Complex III
Mitochondrial-associated membranes

ABSTRACT

Some aquaporins (AQPs) can transport H_2O_2 across membranes, allowing redox signals to proceed in and between cells. Unlike other peroxiporins, human AQP11 is an endoplasmic reticulum (ER)-resident that can conduit H_2O_2 to the cytosol. Here, we show that silencing Ero1α, an ER flavoenzyme that generates abundant H_2O_2 during oxidative folding, causes a paradoxical increase in luminal H_2O_2 levels. The simultaneous AQP11 downregulation prevents this increase, implying that H_2O_2 reaches the ER from an external source(s). Pharmacological inhibition of the electron transport chain reveals that Ero1α downregulation activates superoxide production by complex III. In the intermembrane space, superoxide dismutase 1 generates H_2O_2 that enters the ER channeled by AQP11. Meanwhile, the number of ER-mitochondria contact sites increases as well, irrespective of AQP11 expression. Taken together, our findings identify a novel interorganellar redox response that is activated upon Ero1α downregulation and transfers H_2O_2 from mitochondria to the ER via AQP11.

1. Introduction

The endoplasmic reticulum (ER) is a multifunctional organelle that acts as the cradle for many proteins and lipids, a calcium store, and a central signaling hub. All these systems must act coordinately to preserve functional integrity. A demanding task is to generate and maintain optimal redox conditions for the formation and rearrangement of disulfide bonds in proteins destined to the extracellular space [1,2]. Key in these processes is the ER oxidoreductin 1- protein disulfide isomerase (Ero1-PDI) pathway. Oxidized PDI donates disulfide bonds to newly made cargo proteins and is recharged by the oxidases Ero1α or Ero1β [3,4]. These flavoenzymes can transfer electrons directly to molecular oxygen, generating H_2O_2 as secondary product [5–7]. Besides protein relays capable of precisely targeting redox reactions [8,9], small non-protein thiols and oxidants participate in oxidative folding [10], including H_2O_2 itself [11]. Therefore, not only does the ER environment sustain oxidative folding, but disulfide bond formation itself generates reactive by-products, defining a mutual interdependence [12,13].

Redundant mechanisms allow higher eukaryotes to maintain a cysteine-rich proteome without severe proteostatic problems. For instance, while Ero1 knock-out is lethal in yeast and worms, rather minor phenotypes hallmark mammalian cells and mice [14,15]. Indeed, Prdx4, Gpx7 and Gpx8 are ER-resident enzymes that can use H_2O_2 to oxidize PDI and fuel disulfide bond formation upon Ero1α depletion [13,16–19]. Also NADPH oxidase 4 (NOX4) [20] and VKOR are alternative H_2O_2 producers that could vicariate Ero1α [21]. H_2O_2 molecules produced during oxidative folding -particularly abundant in cells with a robust secretory profile-can be also used as signals, exploiting the steep ER-cytosol gradient [22]. As the ER membrane acts as a barrier against passive diffusion of H_2O_2 [23], channels are needed. One is AQP11, a resident peroxiporin that constitutively transports H_2O_2 outside the ER [22].

Which are the source(s) of the H_2O_2 molecules that reach the cytosol via AQP11? To answer this question, we focused on two main suspects:

Abbreviations: AQP, aquaporin; ER, Endoplasmic Reticulum; Ero1α, ER oxidoreductin 1- α; H_2O_2, Hydrogen Peroxide; MAM, mitochondria-associated ER membranes; NOX, NADPH oxidase; Mfn2, mitofusin-2; PDI, protein disulfide isomerase; SOD1, Superoxide Dismutase 1; VAPB, vesicle-associated membrane protein-associated protein B.

* Corresponding author.
** Corresponding author.
E-mail addresses: imedrano@ing.uc3m.es (I. Medraño-Fernandez), sitia.roberto@hsr.it (R. Sitia).

https://doi.org/10.1016/j.redox.2022.102410
Received 27 June 2022; Received in revised form 12 July 2022; Accepted 12 July 2022
Available online 16 July 2022

NOX4 and Ero1α. Silencing the former slightly decreased H_2O_2 levels in the ER, albeit non significatively. In contrast, a paradoxical increase was observed upon Ero1α downregulation. Our results identify complex III coupled to the SOD1 fraction residing in the mitochondria intermembrane space, as the main source of H_2O_2 molecules that eventually enter the ER via AQP11, facilitated also by tightening of the ER-mitochondria contacts.

2. Materials and methods

2.1. Cell culture and generation of HeLa polyclonal stable cell lines

Stable HeLa transfectants expressing HyPer1 [24] in the ER lumen (*HyPer ER Lumen*) or in the mitochondrial matrix (*HyPer Mito*) were generated as previously described in Refs. [22–25]. Cells were maintained in Dulbecco's modified Eagle's medium (DMEM) + GlutaMAXTM-I medium (Gibco, ThermoFisher) complemented with 10% fetal bovine serum (FBS; EuroClone) and 5 mg/ml penicillin-streptomycin (Lonza).

2.2. Plasmids, siRNAs, and transfection procedures

The plasmid to express a myc-tagged ER-targeted catalase (ER-CAT) was a generous gift of Dr. E. Avezov (University of Cambridge, UK). The *HyPer ER Lumen* plasmid, kindly donated by Drs. E. Margittai and M. Geistz (Semmelweis University, Budapest, Hungary), served as template to generate the H_2O_2-insensitive HyPer vector (*SyPher ER Lumen*) using the primers Fw: AGATGGTCACTCTTTGCGCGAT and Rv: ATCGCGCAAAGAGTGACCATCT and validated by sequencing.

Transient transfections were performed onto 2×10^5 plated HeLa cells using JetPei (Polyplus) and cultured for further 48 h before either immunofluorescence or *HyPer* imaging confocal laser scanning.

The reagents to silence AQP11 (Custom siRNA, 5′-GAGCUUCGCUUGCAAGAAU-3), NOX4 (Custom siRNA, 5'-GCAAGACCUGGUCAGUAUA-3') and Mfn2 (Predesigned siRNA #19262) were purchased from Ambion (Life Technologies), while Ero1α-specific siRNA oligonucleotides (5'-CUGUUUUAAGCCACAGACA-3') and VAPB [26] were obtained from Merck. For silencing experiments 8×10^4 cells were grown in 6-well plates and transfected with 30 pmol of each siRNA for 2 days, using RNAiMAX lipofectamine (Invitrogen) according to the manufacturer's instructions. Silencing efficiency was monitored by real-time PCR as detailed in Ref. [27] using the following primers: AQP11- Fw 5'-TAGCTTGCAGGAATCCCATC-3' and Rv 5'-CTCCTGCATAGGCCAAAAAG-3'; Ero1α- Fw 5'-GTGTGGCTGCTCAGCTCG-3' and Rv 5'-TCAATGGTTTCAAACATCACAGG-3'; NOX4- Fw 5'-AAGACTCCGAAATTCTGCCC-3' and Rv 5'-AACCAACGGAAGGACTGGA-3'; Mfn2- Fw 5'-ATTGCAGAGGCGGTTCGACTCA-3' and Rv 5'-TTCAGTCGGTCTTGCCGCTCTT-3'; VAPB- Fw 5'-AGGTTA TGGAAGAATGTAAGAGGC-3' and Rv 5'-GTTGCTCTGCACTGTCTTCCTC-3'.

2.3. HyPer confocal laser scanning

To perform imaging assays, 8×10^4 HeLa cells stably expressing either *HyPer ER Lumen* or *HyPer Mito* were silenced and/or transfected on 23 mm glass coverslips for 48 h as described above. For analyzing the mitochondrial source of the flux, cells were further treated for the indicated times with 33 μM S3QEL [28] from Sigma, 33 μM S1QEL [29] from Cayman Chemical C. or 2 μM LCS-1 [30] from EMD Millipore, all prepared in DMSO. Time 0 in these experiments corresponds with cells treated only with the vehicle.

After 48 h, cells on coverslips were equilibrated in Ringer buffer (RB: 140 mM NaCl, 2 mM $CaCl_2$, 1 mM $MgSO_4$, 1.5 mM K_2HPO_4, 10 mM Glucose, pH 7.4) for 10min at room temperature before acquisition. Confocal images were collected every 2sec for 1min by dual excitation with 488-nm argon and 405-nm violet diode lasers using an Ultraview confocal laser scanning microscope equipped with an EC Plan - Neofluar 20X (NA 0.45) Dry (Carl Zeiss). To determine the response of a completely reduced probe (Fig. S1A), cells were treated with 5 mM DTT (Sigma) for 5min, recorded for a further minute and then challenged with 50 μM H_2O_2 (Sigma). Each biological condition is represented after averaging 3 technical replicates. For each technical sample, the 488/405-nm ratios were calculated for ≥25 cells using ImageJ, and averaged excluding the initial 20sec of acquisition to allow for laser equilibration. The results are showed as the mean fold change in the basal ratio with respect to controls ± SEM. From 2 to 10 experiments were conducted for each condition assayed.

Representative images of the basal ratio of *HyPer ER Lumen* or *HyPer Mito* were acquired using a GE Healthcare DeltaVisionTM Ultra microscope equipped with a Plan - Apo 60 X (NA 1 0.42) oil objective lens. To this end, 8×10^4 *HyPer ER Lumen*- or *Mito*-expressing HeLa cells were silenced and/or transfected onto coverslips as described above and equilibrated 10min in FluoroBrite DMEM medium (Gibco) with 10% FCS before acquisition.

2.4. Immunofluorescence analyses

To assess the correct localization of the myc-tagged ER-targeted catalase, 8×10^4 Hela cells were plated on 13 mm coverslips placed in 6-well plates and transfected for 48 h. The recombinant protein was detected using in-house generated mouse monoclonal antibodies (9E10, PBS 5% FCS). Rabbit anti-calnexin antibodies (#ADI-SPA-860F, 1 Enzo Life Sciences) were used to decorate the ER. Briefly, cells were fixed with 4%PFA for 20min at room temperature and permeabilized with 0.1% Triton X100 before incubation with the indicated antibodies. Suitable anti-mouse or anti-rabbit secondary antibodies Alexa Fluor-488 and Alexa Fluor-546 (Molecular Probes) were then used, and fluorescent images acquired by a GE Healthcare DeltaVisionTM. Images were processed with ImageJ.

2.5. Transmission electron microscopy

HeLa cells were fixed with 2.5% glutaraldehyde in 0,1 M cacodylate buffer (pH 7.4), washed thoroughly in cacodylate buffer and post-fixed in 1% osmium tetroxide (OsO_4), 1.5% potassium ferricyanide (K_4 [Fe$(CN)_6$]), 0.1 M Na-Cacodylate buffer for 1 h on ice, washed with distilled water (dH_2O) and *enbloc* stained with 0.5% uranyl acetate in dH_2O overnight at 4 °C in the dark. Finally, samples were rinsed in dH_2O, dehydrated with increasing concentrations of ethanol, embedded in Epon, and cured in an oven at 60 °C for 48 h. Ultrathin sections (70–90 nm) were obtained using an ultramicrotome (UC7, Leica microsystem), collected, stained with uranyl acetate and Sato's lead solutions, and observed in a Transmission Electron Microscope Talos L120C (FEI, Thermo Fisher Scientific) operating at 120 kV. Images were acquired with a Ceta CCD camera (FEI, Thermo Fisher Scientific). For morphometric analyses of mitochondria and MAMs, the areas and the perimeters (ROIs) of at least 200 mitochondria per sample were drawn using the freehand selections of ImageJ (n = 3). All ROIs were then extended with the enlarge function and the ER cisternae or tubules present within 30 nm or less from the mitochondria selected were scored as a MAM. GraphPad Prism was used to represent the number of contacts.

2.6. Statistical analyses

We used the one-way ANOVA method for multiple samples and the Tukey's HSD post-hoc test to find out which groups were significantly different from others. In all cases, statistical significance was defined as $p < 0.05$ (*), $p < 0.01$ (**) or $p < 0.001$ (***).

3. Results

3.1. H_2O_2 increases inside the ER upon Ero1α silencing

Stable HeLa transfectants expressing targeted ratiometric *HyPer*

probes [31] allow to reproducibly measure variations in the H_2O_2 levels of the ER lumen despite the high oxidative environment of this organelle (Fig. S1A; [22]). As previously reported [22], AQP11 silencing increased the basal oxidation of *HyPer ER lumen,* likely reflecting the trapping of locally generated H_2O_2 molecules inside the ER. To investigate their main sources, we silenced the expression of Ero1α and NOX4 (Fig. S1B), two ER-resident enzymes known to release H_2O_2 into the lumen [32,33]. NOX4 downregulation caused only a statistically non-significant decrease in the basal H_2O_2 levels (Fig. 1A, green column). In contrast, the results obtained upon Ero1α silencing were most surprising, in that lowering the levels of an oxidase strongly increased the oxidation state of the *HyPer ER lumen* probe (Fig. 1A, red column, and 1B upper panels). Cells stably expressing a pH-insensitive sensor (*SHyPer ER lumen*) did not undergo significant fluorescent shifts, excluding changes in luminal pH (Fig. S1C).

Importantly, simultaneous AQP11 silencing prevented the increase in luminal H_2O_2 observed in cells deprived of Ero1α (Fig. 1A, red and orange-striped column, and 1B upper panels), implying a role for AQP11 in importing H_2O_2 from sources external to the ER. The simultaneous silencing of NOX4 and AQP11 increased the oxidation levels of *HyPer* with respect to single-silencing of NOX4, albeit in a non-significant manner. These results point at Ero1α as the main source of luminal H_2O_2 in untreated HeLa cells (Fig. 1A, green and orange-striped column, and 1B upper panels).

To prove that indeed H_2O_2 accumulates in the ER upon Ero1α or AQP11 downregulation, we co-expressed an ER-targeted catalase (Fig. S1D). As shown in panel B of Fig. 1, the presence of a powerful H_2O_2 scavenger counteracted the increases observed in *HyPer ER lumen* activation, further confirming that the sensor faithfully reports on the H_2O_2 levels in the ER lumen.

The observation that H_2O_2 levels do not increase upon simultaneous AQP11 and Ero1α knockdown confirm that Ero1α is a key source of the H_2O_2 molecules that eventually reach the cytosol via AQP11 [22]. They also imply that –unexpectedly- abundant H_2O_2 molecules enter the ER lumen of cells lacking Ero1α. Thus, an external source is activated upon silencing Ero1α, which generates H_2O_2 molecules that can reach the ER lumen via AQP11.

3.2. H_2O_2 increases also in mitochondria upon Ero1α silencing

In search of the generator(s) of the H_2O_2 detected with *HyPer ER Lumen* when Ero1α was silenced, our suspects fell first on mitochondria. These organelles contain at least 11 different ROS sources [29], establish close contacts with the ER, and are known to exchange other diffusible molecules such as calcium with it [34,35]. Moreover, both AQP11 [22] and Ero1α [36] have been reported to be partially localized in mitochondrial-associated membranes (MAMs).

To explore this possibility, we analyzed HeLa S3 transfectants that stably express *HyPer* in the mitochondrial matrix (*HyPer Mito*). Clearly, also the mitochondrial sensor was oxidized upon Ero1α downregulation (Fig. 2A, red column), mirroring the increase detected in the ER (Fig. 2B, compare middle images). Remarkably, *HyPer Mito* basal oxidation levels did not increase when only AQP11 was silenced, while *HyPer ER lumen* did [22]. Moreover, H_2O_2 levels increased in the mitochondrial matrix also upon combined downregulation of AQP11 and Ero1α (Fig. 2A, red and orange column, and Fig. 2B, right panels). Thus, the peroxiporin activity of AQP11 is not required for *HyPer Mito* oxidation in cells with low Ero1α levels.

3.3. Complex III is activated upon silencing of Ero1α

Amongst the numerous potential H_2O_2 source(s) in mitochondria, site IQ in complex I and site $IIIQ_0$ in complex III stand out for their capacity to produce redox equivalents [37]. Their topology determines the side of the mitochondrial inner membrane (IMM) in which the molecules are produced [38]. Site IQ site produces superoxide ($O_2^{\bullet-}$) and H_2O_2

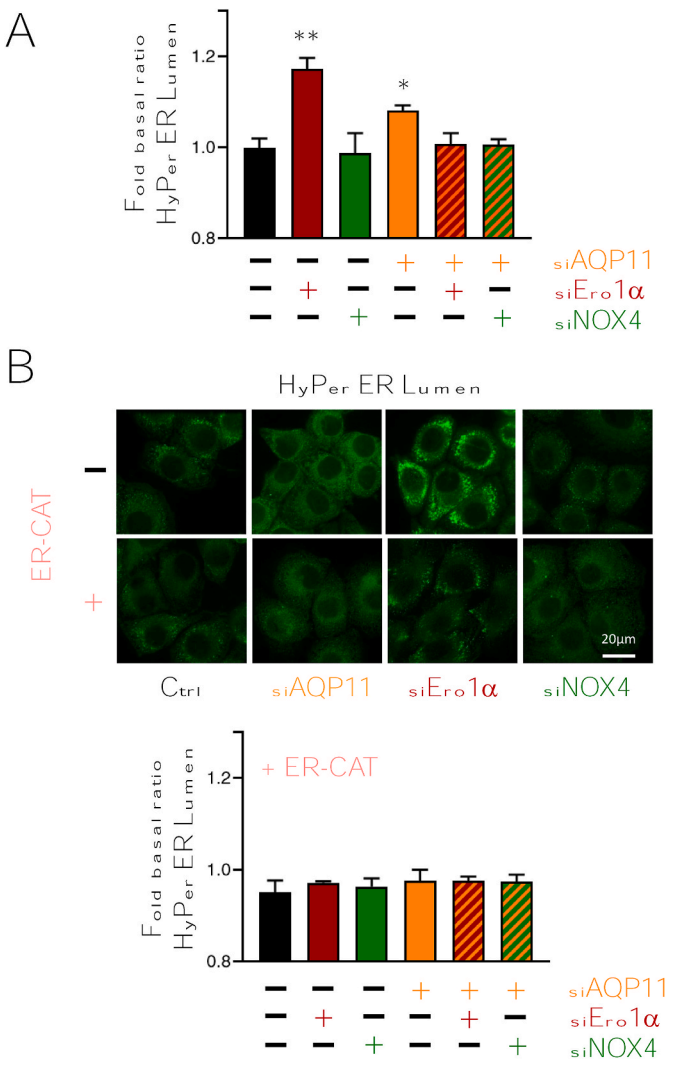

Fig. 1. Ero1α silencing causes a paradoxical increase in the levels of H_2O_2 inside the ER lumen.
A) The graph summarizes the changes induced by the indicated treatments in the basal ratio (488/405) of *HyPer ER Lumen*, expressed in fold change with respect to untreated cells. As previously reported [22], the silencing of AQP11 (orange column) caused an increase in probe oxidation. Downregulation of NOX4, alone or in combination with (green and green-orange striped columns) had effects below the significance levels. In contrast, Ero1α downregulation caused a higher increase in basal *HyPer ER Lumen* oxidation (red column) than AQP11 silencing alone. This increase was abolished when both AQP11 and Ero1α were downregulated (red-orange striped column). Bars represent the average of ≥5 independent experiments ± SEM. P-Value *<0.05 ** < 0.01. B) Expression of catalase in the ER lumen (ER-CAT) abolished the differences observed upon AQP11, Ero1α or NOX4 silencing, confirming that the observed results reflected rises in the luminal concentration of H_2O_2. Average of ≥2 independent experiments ± SEM. P-Value *<0.05 ** < 0.01. The top panels show representative images of HeLa cells expressing *Hyper ER Lumen* under the indicated silencing conditions. The four bottom panels show cells co-expressing ER-catalase. Scale Bar = 20 μm.. (For interpretation of the references to colour in this figure legend, the reader is referred to the Web version of this article.)

inside the matrix (MM, Fig. 3A), the former being transformed into the latter by a matrix superoxide dismutase (MnSOD or SOD2). In contrast, complex III site $IIIQ_0$ releases $O_2^{\bullet-}$ into either side of the IMM (Fig. 3A). In the intermembrane space (IMS), H_2O_2 is generated by cytosolic Cu/ZnSOD or SOD1. To identify the source of H_2O_2 activated in mitochondria upon Ero1α silencing, we selectively blocked electron leakage from site IQ or site $IIIQ_0$ using a new generation of specific inhibitors [39,40]. Unlike classical compounds such as rotenone or antimycin A,

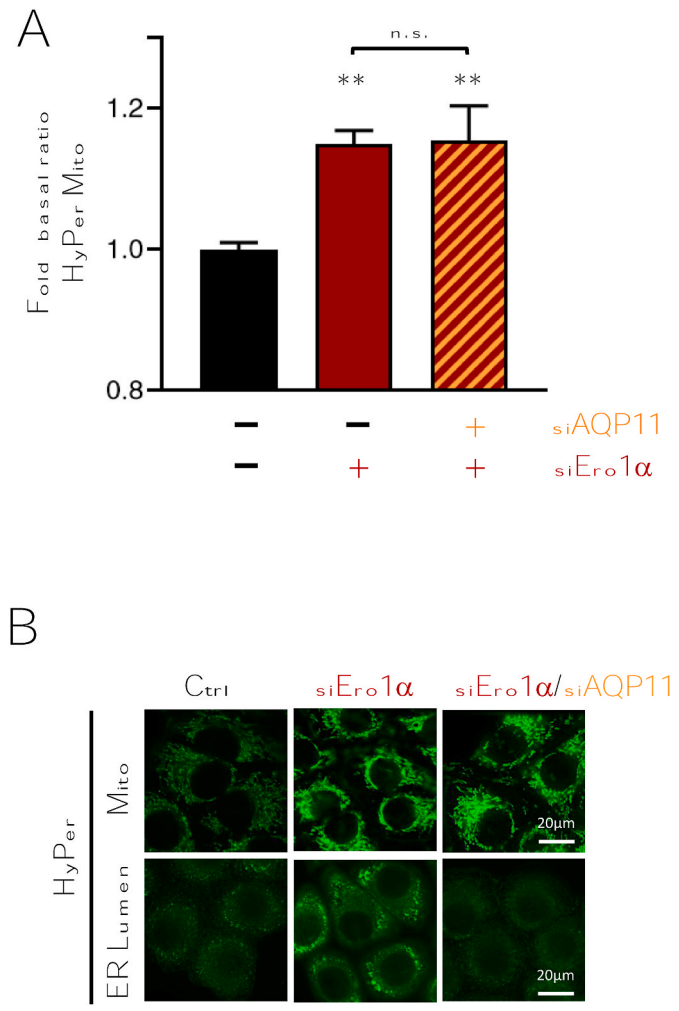

Fig. 2. The H_2O_2 levels increase also in mitochondria upon Ero1α silencing. A) Cells expressing *HyPer* in the mitochondrial matrix were silenced with Ero1α-specific oligos alone or in combination with AQP11-specific reagents, as indicated. Variations in the basal oxidative level of *HyPer Mito* are expressed as fold change relative to untreated cells. Downregulation of Ero1α (siEro1α) favors *HyPer Mito* oxidation (red column) also in cells with low AQP11 activity (red-orange striped column). Bars represent the average of ≥5 independent experiments ± SEM. P-Value **<0.01; n.s. non significant. B) Representative images of *HyPer Mito* and *HyPer ER Lumen* basal fluorescence after the knockdown of Ero1α or Ero1α/AQP11 simultaneously. Scale Bar = 20 μm.. (For interpretation of the references to colour in this figure legend, the reader is referred to the Web version of this article.)

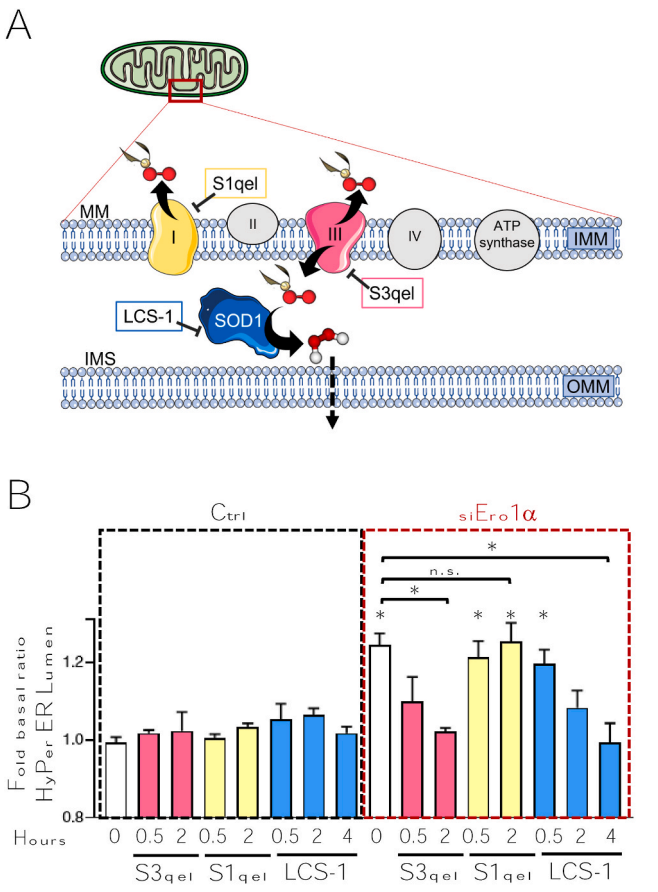

Fig. 3. Complex III is activated upon silencing of Ero1α. A) Schematic representation of the main electron transport chain components present in the inner mitochondrial membrane (IMM). Both complex I and complex III (highlighted in yellow and pink, respectively) produce superoxide. Unlike complex I, however, complex III releases superoxide also in the mitochondrial intermembrane space (IMS). Here, superoxide dismutase 1 (SOD1, in blue) can generate H_2O_2. The boxes indicate the drugs used to specifically inhibit the three activities. B) Time-dependent effects of the S3qel, S1qel and LCS-1 on the basal oxidative level of *HyPer ER Lumen* before (left panel) or after (right panel) Ero1α silencing. The "0" column represents cells treated with the drug vehicle (DMSO). S3qel and S1qel inhibit complex III and complex I (pink and yellow columns, respectively); LCS-1 (blue columns) inhibits SOD1. Average of ≥5 independent experiments ± SEM. P-Value with respect to control is indicated at the top of the significant columns, while statistically significant differences among groups are highlighted with a linker. In all cases P-Value *<0.05 ** < 0.01.. (For interpretation of the references to colour in this figure legend, the reader is referred to the Web version of this article.)

these drugs neither completely interrupt electron flow nor do they alter metabolite consumption. Consequently, they induce fewer compensatory mechanisms from upstream and downstream sites and conserve the membrane potential and ATP production rate, limiting cell toxicity and other potential artefacts [41]. Clearly, the inhibition of site $IIIQ_0$ in complex III by S3qel caused a time-dependent decrease in the levels of H_2O_2 in the ER lumen (Fig. 3B, pink columns). In contrast, inhibiting complex I activity did not significantly affect the luminal levels of H_2O_2 (Fig. 3B, yellow columns). Both compounds lowered the H_2O_2 levels sensed in the mitochondrial matrix by *HyPer Mito*, though to different extents (Fig. S2). Altogether, the above data confirm that lowering the Ero1α levels in the ER induces a higher electron leakage in mitochondria and identifies mitochondrial complex III as the main source of H_2O_2 molecules entering the ER.

To further confirm the above conclusions, we devised a strategy based on the notion that AQPs are not able to transport charged solutes. As stated above, complex III only produces $O_2^{\bullet-}$. Owing to its charged nature, $O_2^{\bullet-}$ cannot be transported across peroxiporins [42]. Therefore, we reasoned that if peroxiporin were needed to mediate H_2O_2 entry into the ER, blockade of SOD1 should prevent *HyPer ER Lumen* oxidation upon Ero1α silencing (see the scheme in Fig. 3A). Accordingly, a pyridazin-3-one derivative (LCS-1), known to effectively inhibit SOD1 activity [43], prevented the H_2O_2 increase in the ER lumen, confirming the requirement of $O_2^{\bullet-}$ transformation into a suitable peroxiporin substrate.

3.4. Reorganization of ER-mitochondria contact sites promotes H_2O_2 transfer upon Ero1α silencing

As effective communication between cellular compartments is facilitated by the vicinity of the organelles involved [44], physical contacts between the ER and mitochondria are emerging as key signaling hubs [35–45]. In the case of H_2O_2, vicinity is of paramount

relevance, as the reactivity of this compound and the abundance of scavenger antioxidants in the cytosol would limit signal diffusion [46,47]. We and others have shown previously that key redox modulators including AQP11 and Ero1α accumulate partly in MAMs [22–34,48,49]. Therefore, we reasoned that the entry of H_2O_2 molecules generated in mitochondria upon Ero1α silencing, would be facilitated by tightening of the ER-mitochondria physical links. To visualize MAMs, we performed systematic morphometric analyses of transmission electron microscopy images (Fig. 4A and B). As there is still controversy on minimal length of the interorganellar interface that can define a MAM from casual contacts between organelles in crowded cells, we selected a stringent gap width threshold for discrimination (≤30 nm) [50]. The results of this endeavor are summarized in panel B of Fig. 4. Clearly, the number of ER-mitochondria contacts was dramatically increased upon Ero1α silencing. Importantly, these were not due to an expansion of mitochondrial dimensions as Ero1α silencing slightly reduced their area (Fig. S3). Simultaneous downregulation of AQP11 neither prevented nor inhibited the effects of Ero1α silencing. Thus, like complex III activation, MAM remodeling can occur also without efficient H_2O_2 transport across the ER membrane. Numerous proteins are thought to dynamically control MAMs [51–53]. To prove that the tightening of the ER-mitochondria contacts observed above was important for H_2O_2 transfer, we silenced the vesicle-associated membrane protein-associated protein B (VAPB), and mitofusin-2 (Mfn2), two proteins known to be essential for correct juxtaposition of the two organelles, despite in different manner [26–54],[55–57]. Clearly, neither VAPB nor Mfn2 silencing impacted the ER H_2O_2 basal levels (Fig. 4C columns pink and purple). However, the increase in H_2O_2 normally observed upon Ero1α downregulation was no longer detectable in cells devoid of VAPB or Mfn2 (Fig. 4C red-pink and red-purple striped columns). These results confirm that the flux of H_2O_2 from mitochondria to ER depends also on the architecture of MAMs.

Taken together, our results show that not only mitochondrial complex III is induced to produce more H_2O_2 in the absence of Ero1α, but MAMs are remodeled to allow efficient ER delivery.

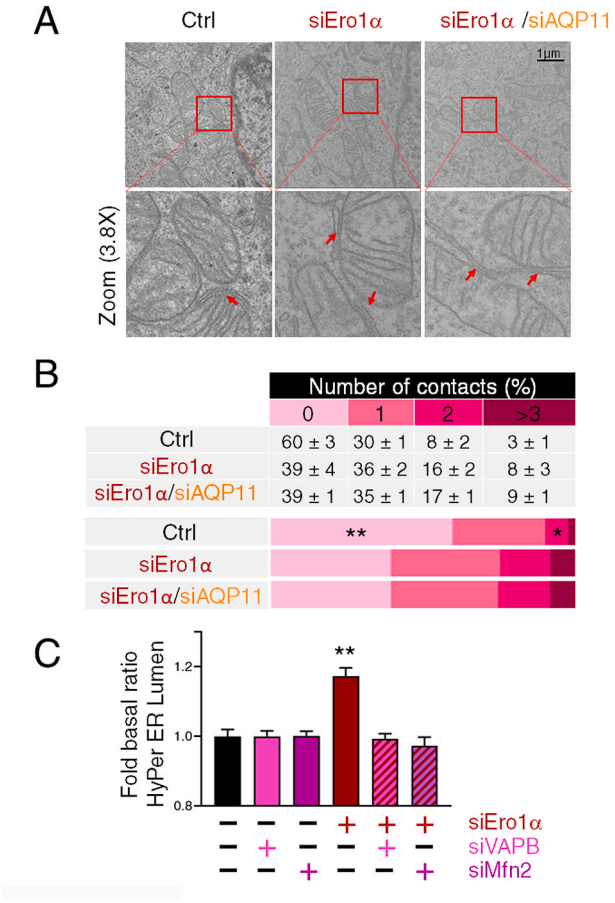

Fig. 4. MAM's reorganization allows H_2O_2 transfer from mitochondria when Ero1α is silenced.
A) Representative transmission electron microscopy images of HeLa cells treated for ≤48 h with the indicated silencing reagents. Scale Bar = 1 μm. Insets are enlarged 3.8 times to better illustrate ER-mitochondria contacts (see red arrows). B) The table shows the average number of contacts that a single mitochondrion establishes with the ER (mitochondria with 0, 1, 2, ≥3 contacts). Mean of three independent experiments, in which at least 200 mitochondria were counted for each condition. The graphs summarize the increase in the number of contacts that mitochondria establish with ER membranes. P-Value *<0.05 ** < 0.01. C) Disturbing the architecture of ER-mitochondria contact sites inhibits H_2O_2 transfer. HeLa cells stably expressing *HyPer ER Lumen* were treated with the indicated oligos to downregulate VAPB (pink column) or Mfn2 (purple column) alone or in combination with Ero1α (red-pink and red-purple striped columns). Clearly, both VAPB and Mfn2 are required for efficient H_2O_2 transfer from mitochondria to the ER lumen in cells with low Ero1α levels (red column). Average of ≥3 independent experiments ± SEM. P-Value *<0.05 ** < 0.01.. (For interpretation of the references to colour in this figure legend, the reader is referred to the Web version of this article.)

4. Discussion

Functional specialization is important for achieving competence in complex societies, but proficiency cannot be reached without distributing responsibilities and emergency plans. Hence, collaborative relationships constitute the basis of successful cohabitation. Clearly, this concept also applies to cells. Compartmentalization of biochemical reactions in membrane-bound organelles has paved the thriving of eukaryotic organisms. Enclosed generation of energy in mitochondria, achievement of intricate protein folds inside the ER [58] and efficient transmission of signals across the cytosol are relevant examples, all sustained by physical isolation of the processes using lipid bilayers. Still, maintenance of cellular homeostasis involves redundancies and interorganellar cooperation via sensors and effector elements that allow survival and adaptation. Our paradoxical finding that inhibiting a powerful source of H_2O_2, Ero1α, increases the H_2O_2 levels in the ER lumen is to be seen in this context, as adequate safeguarding responses must be readily available when key players are compromised. Gradients must be generated and maintained across membranes [59–61] and channels gated in a timely and spatially regulated manner [25–46],[61,62].

The notion that Ero1α generates H_2O_2 during disulfide bond formation links oxidative folding to redox signaling. Thus, H_2O_2 molecules flow from the ER to the cytosol via the peroxiporin AQP11 [22], conceivably yielding information on the rate of protein biogenesis within the secretory compartment. Our experiments reveal that NOX4 is a minor source of luminal H_2O_2, a role played by Ero1α also in non-professional secretory cells like HeLa. Not only does Ero1α provide most luminal H_2O_2, it also ensures that H_2O_2 levels be restored in its absence, asking and obtaining help from mitochondrial complex III (Fig. 5).

In all likelihood, the process we describe here is important in maintaining redox homeostasis in an ER deprived of a key player. The teleology of having closer contacts between mitochondria and the ER is therefore clear, especially considering the abundance of antioxidants in the cytosol. It would be of great interest to identify the mechanisms that tether the two organelles and regulate the intervening distances. That Ero1α is involved in tight relationships with mitochondria does not come as a surprise. In fact, we and others have previously shown that its levels impact calcium fluxes [35–64]. How can the absence of a soluble enzyme in the ER lumen be perceived by complex III in the inner mitochondrial membrane? Since the *HyPer Mito* sensor is activated upon Ero1α silencing also when H_2O_2 export via AQP11 is inhibited, H_2O_2 is unlikely to be involved. The nature of the messages remains to be

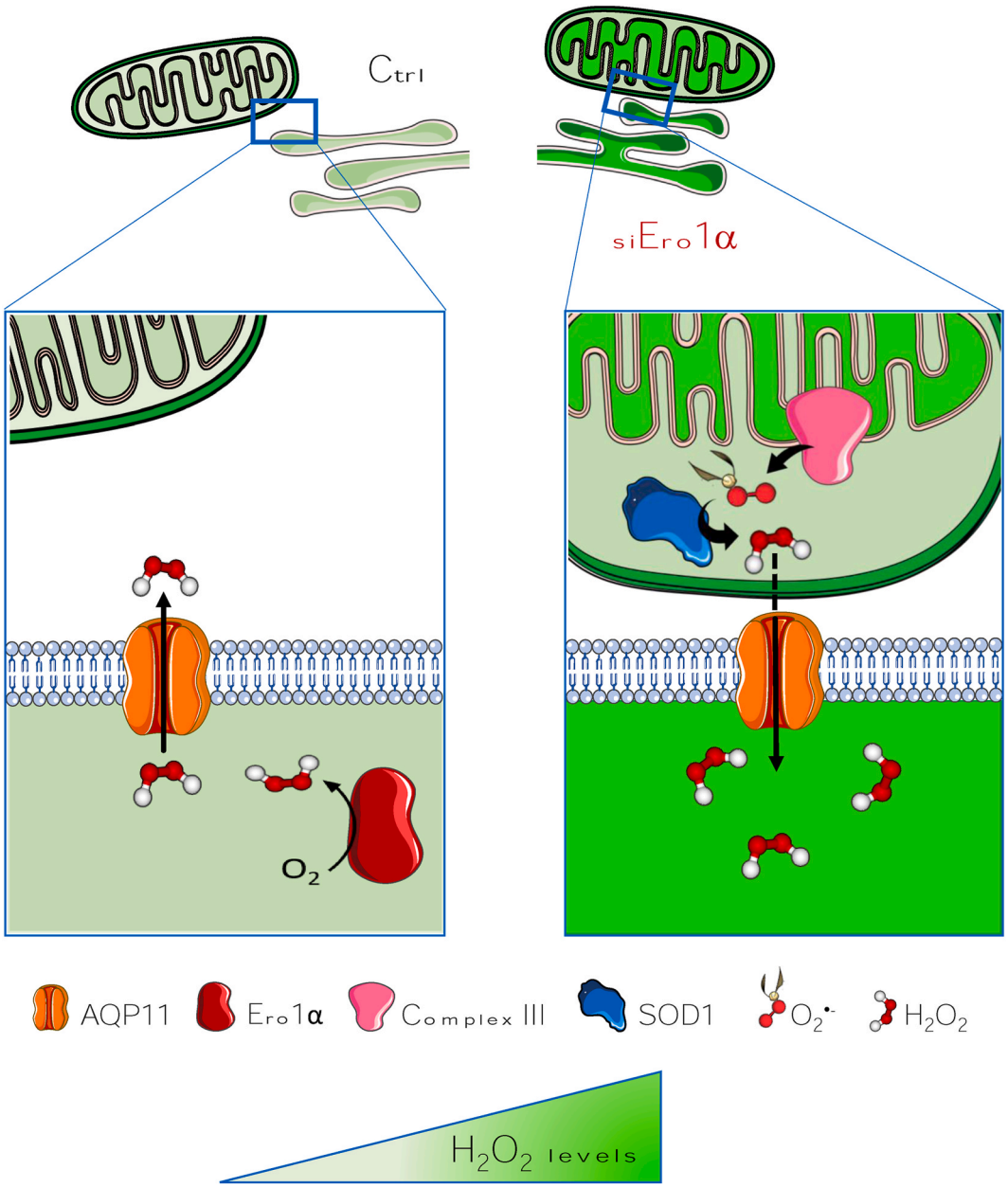

Fig. 5. Model of the Ero1α-AQP11 signaling pathway.
In resting HeLa cells (left panel), H_2O_2 leaves the ER and reaches the cytosol via AQP11 [22]. Upon Ero1α silencing, complex III (pink) produces more superoxide in the IMS, which is converted by SOD1. H_2O_2 eventually enters the ER via AQP11, presumably due to the augmented contacts with the ER (right panel). The different green intensity in mitochondrial matrix and ER lumen summarizes the observed changes in HyPer basal oxidation states. . (For interpretation of the references to colour in this figure legend, the reader is referred to the Web version of this article.)

established, calcium ions [48–49][63], and oxygen molecules [65–68] being reasonable candidates.

As it is often the case with novel findings, our study raises more questions than it answers. The notion that Ero1α levels impact the activity of complex III in mitochondria as well as the anatomy of the organelles involved highlights once more how all the ingredients in our cells operate in a synergic fashion to guarantee survival also in dire conditions. Dissecting the underlying mechanisms is bound to identify key targets in a wide spectrum of pathophysiologic conditions.

Funding

This work was supported through grants from the Associazione Italiana Ricerca sul Cancro (IG 2019–23285 to R.S.) and Ministero dell'Istruzione, dell'Università e della Ricerca (MIUR)-PRIN (grant no. 2017XA5J5N). I.M.-F. was supported by the Madrid Government (Comunidad de Madrid) under the Multiannual Agreement with UC3M in the line of "Research Funds for Beatriz Galindo Fellowships" (REDOXSKIN-CM-UC3M), and in the context of the V PRICIT (Regional Programme of Research and Technological Innovation", and by "Proyectos de I + D + I" (PID2020-114230 GA-I00 to I.M.-F.) funded by MCIN/AEI/10.13039/501100011033/. MG was supported by the European Union's Horizon 2020 research and innovation programme under the Marie Skłodowska-Curie grant agreement No 754432 and the Polish Ministry of Science and Higher Education, from financial resources for science in 2018–2023 granted for the implementation of an international co-financed project.

Author contributions

I.M-F., I.S. and R.S. designed the strategy of the study. I.S. performed most experiments, while M.G. contributed in the initial ratio analyses and RT-PCR assays. Andrea Raimondi from the Alembic Facilities performed EM images while analyses were made by IS. All authors contributed in interpreting the data. I.S., R.S. and I.M.-F. wrote the manuscript.

Data and materials availability

Most data needed to evaluate the conclusions in the study are present in the text, figures and supplementary materials. Raw data may be obtained upon request.

Declaration of competing interest

The authors declare no competing interests.

Data availability

The data that has been used is confidential.

Acknowledgements

In addition to all members of our laboratories, we thank L. Rampoldi, A. Rubartelli, E. van Anken and L. Cassina (San Raffaele Scientific Institute, Milan, Italy), Paola Pizzo (University of Padova, Italy), G.P. Bienert (Technical University of Munich, Germany) and S. Bestetti and T. Simmen (University of Alberta, Canada) for useful suggestions, exciting discussions, and constructive criticisms. IS thanks V. Belousov for being her most helpful external PhD supervisor. Part of this work was carried out in the Advanced Light and Electron Microscopy BioImaging Center (ALEMBIC) of San Raffaele Scientific Institute and Vita-Salute University to which staff -particularly Dr. A. Raimondi who performed the electron microscopy assays-we are profoundly grateful.

We are indebted with Drs. E. Avezov (University of Cambridge, UK), V. Belousov (Institute of Bioorganic Chemistry, Moscow, Russia), E. Margittai and M. Geistz (Semmelweis University, Budapest, Hungary), L. Cassina (San Raffaele Scientific Institute, Milan, Italy) for providing plasmids and reagents. Because of space limitations, we apologize to all those colleagues and researchers in the field whose work is not directly cited here.

Appendix A. Supplementary data

Supplementary data to this article can be found online at https://doi.org/10.1016/j.redox.2022.102410.

References

[1] A.R. Frand, J.W. Cuozzo, C.A. Kaiser, Pathways for protein disulphide bond formation, Trends Cell Biol. 10 (2000) 203–210, https://doi.org/10.1016/s0962-8924(00)01745-1.

[2] K.M. Holmström, T. Finkel, Cellular mechanisms and physiological consequences of redox-dependent signalling, Nat. Rev. Mol. Cell Biol. 15 (2014) 411–421, https://doi.org/10.1038/nrm3801.

[3] A. Cabibbo, M. Pagani, M. Fabbri, M. Rocchi, M.R. Farmery, N.J. Bulleid, R. Sitia, ERO1-L, a human protein that favors disulfide bond formation in the endoplasmic reticulum, J. Biol. Chem. 275 (2000) 4827–4833, https://doi.org/10.1074/jbc.275.7.4827.

[4] M. Pagani, M. Fabbri, C. Benedetti, A. Fassio, S. Pilati, N.J. Bulleid, A. Cabibbo, R. Sitia, Endoplasmic reticulum oxidoreductin 1-lbeta (ERO1-Lbeta), a human gene induced in the course of the unfolded protein response, J. Biol. Chem. 275 (2000) 23685–23692, https://doi.org/10.1074/jbc.M003061200.

[5] L. Wang, S. Li, A. Sidhu, L. Zhu, Y. Liang, R.B. Freedman, C. Wang, Reconstitution of human ero1-lα/protein-disulfide isomerase oxidative folding pathway in vitro: POSITION-dependent differences in role between the a and a′ domains of PROTEIN-DISULFIDE isomerase, J. Biol. Chem. 284 (2009) 199–206, https://doi.org/10.1074/jbc.M806645200.

[6] M. Bader, W. Muse, D.P. Ballou, C. Gassner, J.C.A. Bardwell, Oxidative protein folding is driven by the electron transport system, Cell 98 (1999) 217–227, https://doi.org/10.1016/S0092-8674(00)81016-8.

[7] B.P. Tu, J.S. Weissman, The FAD- and O2-dependent reaction cycle of ero1-mediated oxidative protein folding in the endoplasmic reticulum, Mol. Cell 10 (2002) 983–994, https://doi.org/10.1016/S1097-2765(02)00696-2.

[8] E. Vitu, S. Kim, C.S. Sevier, O. Lutzky, N. Heldman, M. Bentzur, T. Unger, M. Yona, C.A. Kaiser, D. Fass, Oxidative activity of yeast Ero1p on protein disulfide isomerase and related oxidoreductases of the endoplasmic reticulum, J. Biol. Chem. 285 (2010) 18155–18165, https://doi.org/10.1074/jbc.M109.064931.

[9] A. Alon, I. Grossman, Y. Gat, V.K. Kodali, F. DiMaio, T. Mehlman, G. Haran, D. Baker, C. Thorpe, D. Fass, The dynamic disulphide relay of quiescin sulphydryl oxidase, Nature 488 (2012) 414–418, https://doi.org/10.1038/nature11267.

[10] H. Christopher, S.A. J, L.H. F, Oxidized redox state of glutathione in the endoplasmic reticulum, Science 257 (1992) 1496–1502, https://doi.org/10.1126/science.1523409.

[11] A.-R. Karala, A.-K. Lappi, M.J. Saaranen, L.W. Ruddock, Efficient peroxide-mediated oxidative refolding of a protein at physiological pH and implications for oxidative folding in the endoplasmic reticulum, Antioxidants Redox Signal. 11 (2009) 963–970, https://doi.org/10.1089/ars.2008.2326.

[12] S. Chakravarthi, N.J. Bulleid, Glutathione is required to regulate the formation of native disulfide bonds within proteins entering the secretory pathway, J. Biol. Chem. 279 (2004) 39872–39879, https://doi.org/10.1074/jbc.M406912200.

[13] T.J. Tavender, N.J. Bulleid, Molecular mechanisms regulating oxidative activity of the Ero1 family in the endoplasmic reticulum, Antioxidants Redox Signal. 13 (2010) 1177–1187, https://doi.org/10.1089/ars.2010.3230.

[14] E. Zito, K.-T. Chin, J. Blais, H.P. Harding, D. Ron, ERO1-beta, a pancreas-specific disulfide oxidase, promotes insulin biogenesis and glucose homeostasis, J. Cell Biol. 188 (2010) 821–832, https://doi.org/10.1083/jcb.200911086.

[15] É. Margittai, R. Sitia, Oxidative protein folding in the secretory pathway and redox signaling across compartments and cells, Traffic 12 (2011) 1–8, https://doi.org/10.1111/j.1600-0854.2010.01108.x.

[16] T.J. Tavender, A.M. Sheppard, N.J. Bulleid, Peroxiredoxin IV is an endoplasmic reticulum-localized enzyme forming oligomeric complexes in human cells, Biochem. J. 411 (2008) 191–199, https://doi.org/10.1042/BJ20071428.

[17] V.D. Nguyen, M.J. Saaranen, A.-R. Karala, A.-K. Lappi, L. Wang, I.B. Raykhel, H. I. Alanen, K.E.H. Salo, C.-C. Wang, L.W. Ruddock, Two endoplasmic reticulum PDI peroxidases increase the efficiency of the use of peroxide during disulfide bond formation, J. Mol. Biol. 406 (2011) 503–515, https://doi.org/10.1016/j.jmb.2010.12.039.

[18] E. Varone, A. Decio, A. Chernorudskiy, L. Minoli, L. Brunelli, F. Ioli, A. Piotti, R. Pastorelli, M. Fratelli, M. Gobbi, R. Giavazzi, E. Zito, The ER stress response mediator ERO1 triggers cancer metastasis by favoring the angiogenic switch in hypoxic conditions, Oncogene 40 (2021) 1721–1736, https://doi.org/10.1038/s41388-021-01659-y.

[19] T. Konno, E. Pinho Melo, C. Lopes, I. Mehmeti, S. Lenzen, D. Ron, E. Avezov, ERO1-independent production of H2O2 within the endoplasmic reticulum fuels Prdx4-mediated oxidative protein folding, J. Cell Biol. 211 (2015) 253–259, https://doi.org/10.1083/jcb.201506123.

[20] F.R.M. Laurindo, T.L.S. Araujo, T.B. Abrahão, Nox NADPH oxidases and the endoplasmic reticulum, Antioxidants Redox Signal. 20 (2014) 2755–2775, https://doi.org/10.1089/ars.2013.5605.

[21] L.A. Rutkevich, D.B. Williams, Vitamin K epoxide reductase contributes to protein disulfide formation and redox homeostasis within the endoplasmic reticulum, Mol. Biol. Cell 23 (2012) 2017, https://doi.org/10.1091/mbc.E12-02-0102. –2027.

[22] S. Bestetti, M. Galli, I. Sorrentino, P. Pinton, A. Rimessi, R. Sitia, I. Medraño-Fernandez, Human aquaporin-11 guarantees efficient transport of H(2)O(2) across the endoplasmic reticulum membrane, Redox Biol. 28 (2020), 101326, https://doi.org/10.1016/j.redox.2019.101326.

[23] M. Csala, É. Kereszturi, J. Mandl, G. Bánhegyi, The endoplasmic reticulum as the extracellular space inside the cell: role in protein folding and glycosylation, Antioxidants Redox Signal. 16 (2011) 1100–1108, https://doi.org/10.1089/ars.2011.4227.

[24] V. v Belousov, A.F. Fradkov, K.A. Lukyanov, D.B. Staroverov, K.S. Shakhbazov, A. v Terskikh, S. Lukyanov, Genetically encoded fluorescent indicator for intracellular hydrogen peroxide, Nat. Methods 3 (2006) 281–286, https://doi.org/10.1038/nmeth866.

[25] I. Medraño-Fernandez, S. Bestetti, M. Bertolotti, G.P. Bienert, C. Bottino, U. Laforenza, A. Rubartelli, R. Sitia, Stress regulates aquaporin-8 permeability to impact cell growth and survival, Antioxidants Redox Signal. 24 (2016) 1031–1044, https://doi.org/10.1089/ars.2016.6636.

[26] P. Gómez-Suaga, B.G. Pérez-Nievas, E.B. Glennon, D.H.W. Lau, S. Paillusson, G. M. Mórotz, T. Calì, P. Pizzo, W. Noble, C.C.J. Miller, The VAPB-PTPIP51 endoplasmic reticulum-mitochondria tethering proteins are present in neuronal synapses and regulate synaptic activity, Acta Neuropathol. Commun. 7 (2019) 35, https://doi.org/10.1186/s40478-019-0688-4.

[27] T. Anelli, M. Dalla Torre, E. Borini, E. Mangini, A. Ulisse, C. Semino, R. Sitia, P. Panina-Bordignon, Profound architectural and functional readjustments of the secretory pathway in decidualization of endometrial stromal cells, Traffic 23 (2022) 4–20, https://doi.org/10.1111/tra.12822.

[28] A.L. Orr, L. Vargas, C.N. Turk, J.E. Baaten, J.T. Matzen, V.J. Dardov, S.J. Attle, J. Li, D.C. Quackenbush, R.L.S. Goncalves, I. V Perevoshchikova, H.M. Petrassi, S. L. Meeusen, E.K. Ainscow, M.D. Brand, Suppressors of superoxide production from mitochondrial complex III, Nat. Chem. Biol. 11 (2015) 834–836, https://doi.org/10.1038/nchembio.1910.

[29] M.D. Brand, Mitochondrial generation of superoxide and hydrogen peroxide as the source of mitochondrial redox signaling, Free Radic. Biol. Med. 100 (2016) 14–31, https://doi.org/10.1016/j.freeradbiomed.2016.04.001.
[30] T. Du, Y. Song, A. Ray, D. Chauhan, K.C. Anderson, Proteomic analysis identifies mechanism(s) of overcoming bortezomib resistance via targeting ubiquitin receptor Rpn13, Leukemia 35 (2021) 550–561, https://doi.org/10.1038/s41375-020-0865-2.
[31] V. V Belousov, A.F. Fradkov, K.A. Lukyanov, D.B. Staroverov, K.S. Shakhbazov, A. V Terskikh, S. Lukyanov, Genetically encoded fluorescent indicator for intracellular hydrogen peroxide, Nat. Methods 3 (2006) 281–286, https://doi.org/10.1038/nmeth866.
[32] Y. Nisimoto, H.M. Jackson, H. Ogawa, T. Kawahara, J.D. Lambeth, Constitutive NADPH-dependent electron transferase activity of the Nox4 dehydrogenase domain, Biochemistry 49 (2010) 2433–2442, https://doi.org/10.1021/bi9022285.
[33] Y. Nisimoto, B.A. Diebold, D. Cosentino-Gomes, J.D. Lambeth, Nox4: a hydrogen peroxide-generating oxygen sensor, Biochemistry 53 (2014) 5111–5120, https://doi.org/10.1021/bi500331y.
[34] T. Anelli, L. Bergamelli, E. Margittai, A. Rimessi, C. Fagioli, A. Malgaroli, P. Pinton, M. Ripamonti, R. Rizzuto, R. Sitia, Ero1α regulates Ca(2+) fluxes at the endoplasmic reticulum-mitochondria interface (MAM), Antioxidants Redox Signal. 16 (2012) 1077–1087, https://doi.org/10.1089/ars.2011.4004.
[35] D.M. Booth, B. Enyedi, M. Geiszt, P. Várnai, G. Hajnóczky, Redox nanodomains are induced by and control calcium signaling at the ER-mitochondrial interface, Mol. Cell 63 (2016) 240–248, https://doi.org/10.1016/j.molcel.2016.05.040.
[36] A.M. Benham, M. van Lith, R. Sitia, I. Braakman, Ero1-PDI interactions, the response to redox flux and the implications for disulfide bond formation in the mammalian endoplasmic reticulum, Phil. Trans. Roy. Soc. Lond. B Biol. Sci. 368 (2013), 20110403, https://doi.org/10.1098/rstb.2011.0403.
[37] M.D. Brand, The sites and topology of mitochondrial superoxide production, Exp. Gerontol. 45 (2010) 466–472, https://doi.org/10.1016/j.exger.2010.01.003.
[38] C.L. Quinlan, I. V Perevoshchikova, M. Hey-Mogensen, A.L. Orr, M.D. Brand, Sites of reactive oxygen species generation by mitochondria oxidizing different substrates, Redox Biol. 1 (2013) 304–312, https://doi.org/10.1016/j.redox.2013.04.005.
[39] A.L. Orr, D. Ashok, M.R. Sarantos, T. Shi, R.E. Hughes, M.D. Brand, Inhibitors of ROS production by the ubiquinone-binding site of mitochondrial complex I identified by chemical screening, Free Radic. Biol. Med. 65 (2013) 1047–1059, https://doi.org/10.1016/j.freeradbiomed.2013.08.170.
[40] A.L. Orr, L. Vargas, C.N. Turk, J.E. Baaten, J.T. Matzen, V.J. Dardov, S.J. Attle, J. Li, D.C. Quackenbush, R.L.S. Goncalves, I. V Perevoshchikova, H.M. Petrassi, S. L. Meeusen, E.K. Ainscow, M.D. Brand, Suppressors of superoxide production from mitochondrial complex III, Nat. Chem. Biol. 11 (2015) 834–836, https://doi.org/10.1038/nchembio.1910.
[41] R.L.S. Goncalves, M.A. Watson, H.-S. Wong, A.L. Orr, M.D. Brand, The use of site-specific suppressors to measure the relative contributions of different mitochondrial sites to skeletal muscle superoxide and hydrogen peroxide production, Redox Biol. 28 (2020), 101341, https://doi.org/10.1016/j.redox.2019.101341.
[42] M.N. Möller, E. Cuevasanta, F. Orrico, A.C. Lopez, L. Thomson, A. Denicola, Diffusion and transport of reactive species across cell membranes, Adv. Exp. Med. Biol. 1127 (2019) 3–19, https://doi.org/10.1007/978-3-030-11488-6_1.
[43] R. Somwar, H. Erdjument-Bromage, E. Larsson, D. Shum, W.W. Lockwood, G. Yang, C. Sander, O. Ouerfelli, P.J. Tempst, H. Djaballah, H.E. Varmus, Superoxide dismutase 1 (SOD1) is a target for a small molecule identified in a screen for inhibitors of the growth of lung adenocarcinoma cell lines, Proc. Natl. Acad. Sci. U. S. A 108 (2011) 16375–16380, https://doi.org/10.1073/pnas.1113554108.
[44] G. Csordás, D. Weaver, G. Hajnóczky, Endoplasmic reticulum–mitochondrial contactology: structure and signaling functions, Trends Cell Biol. 28 (2018) 523–540, https://doi.org/10.1016/j.tcb.2018.02.009.
[45] M. Giacomello, L. Pellegrini, The coming of age of the mitochondria–ER contact: a matter of thickness, Cell Death Differ. 23 (2016) 1417–1427, https://doi.org/10.1038/cdd.2016.52.
[46] D.E. Nordzieke, I. Medraño-Fernandez, The plasma membrane: a platform for intra- and intercellular redox signaling, Antioxidants 7 (2018), https://doi.org/10.3390/antiox7110168.
[47] H. Sies, D.P. Jones, Reactive oxygen species (ROS) as pleiotropic physiological signalling agents, Nat. Rev. Mol. Cell Biol. 21 (2020) 363–383, https://doi.org/10.1038/s41580-020-0230-3.
[48] S.Y. Gilady, M. Bui, E.M. Lynes, M.D. Benson, R. Watts, J.E. Vance, T. Simmen, Ero1alpha requires oxidizing and normoxic conditions to localize to the mitochondria-associated membrane (MAM), Cell Stress Chaperones 15 (2010) 619–629, https://doi.org/10.1007/s12192-010-0174-1.
[49] T. Gutiérrez, H. Qi, M.C. Yap, N. Tahbaz, L.A. Milburn, E. Lucchinetti, P.-H. Lou, M. Zaugg, P.G. LaPointe, P. Mercier, M. Overduin, H. Bischof, S. Burgstaller, R. Malli, K. Ballanyi, J. Shuai, T. Simmen, The ER chaperone calnexin controls mitochondrial positioning and respiration, Sci. Signal. 13 (2020), https://doi.org/10.1126/scisignal.aax6660.
[50] A. Bononi, S. Missiroli, F. Poletti, J.M. Suski, C. Agnoletto, M. Bonora, E. De Marchi, C. Giorgi, S. Marchi, S. Patergnani, A. Rimessi, M.R. Wieckowski, P. Pinton, Mitochondria-associated membranes (MAMs) as hotspot Ca(2+) signaling units, Adv. Exp. Med. Biol. 740 (2012) 411–437, https://doi.org/10.1007/978-94-007-2888-2_17.
[51] M.S. Herrera-Cruz, T. Simmen, Of yeast, mice and men: MAMs come in two flavors, Biol. Direct 12 (2017) 3, https://doi.org/10.1186/s13062-017-0174-5.
[52] T. Simmen, E.M. Lynes, K. Gesson, G. Thomas, Oxidative protein folding in the endoplasmic reticulum: tight links to the mitochondria-associated membrane (MAM), Biochim. Biophys. Acta 1798 (2010) 1465–1473, https://doi.org/10.1016/j.bbamem.2010.04.009.
[53] Y. Fan, T. Simmen, Mechanistic connections between endoplasmic reticulum (ER) redox control and mitochondrial metabolism, Cells (2019) 8, https://doi.org/10.3390/cells8091071.
[54] S. Han, F. Zhao, J. Hsia, X. Ma, Y. Liu, S. Torres, H. Fujioka, X. Zhu, The role of Mfn2 in the structure and function of endoplasmic reticulum-mitochondrial tethering in vivo, J. Cell Sci. 134 (2021) jcs253443, https://doi.org/10.1242/jcs.253443.
[55] O.M. de Brito, L. Scorrano, Mitofusin 2 tethers endoplasmic reticulum to mitochondria, Nature 456 (2008) 605–610, https://doi.org/10.1038/nature07534.
[56] K.J. de Vos, G.M. Mórotz, R. Stoica, E.L. Tudor, K.-F. Lau, S. Ackerley, A. Warley, C. E. Shaw, C.C.J. Miller, VAPB interacts with the mitochondrial protein PTPIP51 to regulate calcium homeostasis, Hum. Mol. Genet. 21 (2012) 1299–1311, https://doi.org/10.1093/hmg/ddr559.
[57] R. Filadi, D. Pendin, P. Pizzo, Mitofusin 2: from functions to disease, Cell Death Dis. 9 (2018) 330, https://doi.org/10.1038/s41419-017-0023-6.
[58] C. Giannone, M.R. Chelazzi, A. Orsi, T. Anelli, T. Nguyen, J. Buchner, R. Sitia, Biogenesis of secretory immunoglobulin M requires intermediate non-native disulfide bonds and engagement of the protein disulfide isomerase ERp44, EMBO J. 41 (2022), e108518, https://doi.org/10.15252/embj.2021108518.
[59] S.G. Rhee, Redox signaling: hydrogen peroxide as intracellular messenger, Exp. Mol. Med. 31 (1999) 53–59, https://doi.org/10.1038/emm.1999.9.
[60] H.A. Woo, S.H. Yim, D.H. Shin, D. Kang, D.-Y. Yu, S.G. Rhee, Inactivation of peroxiredoxin I by phosphorylation allows localized H(2)O(2) accumulation for cell signaling, Cell 140 (2010) 517–528, https://doi.org/10.1016/j.cell.2010.01.009.
[61] T.-C. Meng, T. Fukada, N.K. Tonks, Reversible oxidation and inactivation of protein tyrosine phosphatases in vivo, Mol. Cell 9 (2002) 387–399, https://doi.org/10.1016/s1097-2765(02)00445-8.
[62] S. Bestetti, I. Medraño-Fernandez, M. Galli, M. Ghitti, G.P. Bienert, G. Musco, A. Orsi, A. Rubartelli, R. Sitia, A persulfidation-based mechanism controls aquaporin-8 conductance, Sci. Adv. 4 (2018), https://doi.org/10.1126/sciadv.aar5770 eaar5770.
[63] T. Anelli, L. Bergamelli, E. Margittai, A. Rimessi, C. Fagioli, A. Malgaroli, P. Pinton, M. Ripamonti, R. Rizzuto, R. Sitia, Ero1α regulates Ca2+ fluxes at the endoplasmic reticulum–mitochondria interface (MAM), Antioxidants Redox Signal. 16 (2011) 1077–1087, https://doi.org/10.1089/ars.2011.4004.
[64] E.D. Yoboue, R. Sitia, T. Simmen, Redox crosstalk at endoplasmic reticulum (ER) membrane contact sites (MCS) uses toxic waste to deliver messages, Cell Death Dis. 9 (2018) 331, https://doi.org/10.1038/s41419-017-0033-4.
[65] B. Gess, K.-H. Hofbauer, R.H. Wenger, C. Lohaus, H.E. Meyer, A. Kurtz, The cellular oxygen tension regulates expression of the endoplasmic oxidoreductase ERO1-Lalpha, Eur. J. Biochem. 270 (2003) 2228–2235, https://doi.org/10.1046/j.1432-1033.2003.03590.x.
[66] R.D. Guzy, P.T. Schumacker, Oxygen sensing by mitochondria at complex III: the paradox of increased reactive oxygen species during hypoxia, Exp. Physiol. 91 (2006) 807–819, https://doi.org/10.1113/expphysiol.2006.033506.
[67] N.S. Chandel, Mitochondrial complex III: an essential component of universal oxygen sensing machinery? Respir. Physiol. Neurobiol. 174 (2010) 175–181, https://doi.org/10.1016/j.resp.2010.08.004.
[68] A. Moilanen, K. Korhonen, M.J. Saaranen, L.W. Ruddock, Molecular analysis of human Ero1 reveals novel regulatory mechanisms for oxidative protein folding, Life science alliance 1 (2018), https://doi.org/10.26508/lsa.201800090 e201800090–e201800090.